Combining Energy Harvesting and Cooperative Communications for Low-Power Wide-Area Systems

Xuan Nam Tran, Van-Phuc Hoang, Ba Cao Nguyen

Abstract

This paper presents the combination of energy harvesting (EH) at the wireless sensor and cooperative communications for low-power wide-area (LPWA) systems. Firstly, the Internet of Things sensor harvests the energy from the power beacon with multiple transmit antennas via radio frequency signals and then uses the harvested energy to transmit signals to multiple gateways with multiple receive antennas. Then, the cooperative communication is applied at the server based on the gateway outputs. By mathematical analysis, we derive the exact closed-form expressions of outage probabilities (OPs), throughput, and symbol error probabilities (SEPs) of the EH-LPWA system over the Rayleigh fading channel in the cases without and with cooperative communications. Our expressions can be considered as the first results applying EH for LPWA systems with mathematical analysis. Numerical results have clarified that the distances, path loss exponent, and data transmission rate have a strong impact on the OPs, throughput, and SEPs. Particularly, using half of transmission blocks for EH can maximize the system performance. Moreover, when the number of transmit antennas at the power beacon is equal to the number of receive antennas at gateways, the system performance can be improved significantly. Finally, the accuracy of the obtained expressions is demonstrated via Monte-Carlo simulations.

Index Terms

Low-power wide-area network, long range, energy harvesting, cooperative communication, outage probability, throughput, symbol error probability.

I. Introduction

Recently, energy harvesting (EH) from radio frequency (RF) signals has been widely used to satisfy the energy requirements of wireless communication systems. Hence, it becomes a promising forthcoming technique to be deployed in the fifth generation

Xuan Nam Tran, Van-Phuc Hoang, are with Le Quy Don Technical University, Ha Noi, Vietnam (e-mails: namtx@lqdtu.edu.vn, phuchv@lqdtu.edu.vn).

Ba Cao Nguyen is with Telecommunications University, Khanh Hoa, Vietnam (e-mail: nguyenbacao@tcu.edu.vn).

Corresponding author should be addressed to Van-Phuc Hoang

(5G) and beyond networks [1], [2]. Specifically, EH can supply enough power for sensors in the Internet of Things (IoT) systems, heterogeneous networks (HetNets), mobile devices, and extremely remote area communications. In addition, wireless devices can transmit the RF signals over the air for a long range (LoRa), thus, EH from RF signals can be applied for various devices that are located in the restricted areas, where the traditional energy grid is extremely difficult to be deployed. Consequently, the researches and experiments about EH are fast developed to soon apply this technique for the current and future wireless systems [3]–[5].

In the literature, the linear and non-linear energy harvesters have been proposed to apply EH technique for wireless devices [1], [6]. In particular, the wireless devices can harvest the energy from base stations [7]–[9] or from power beacons [10]. The mathematical analysis was used to derive the expressions in terms of outage probability (OP), throughput, and symbol error probability (SEP) of the EH communication systems [7], [10]. It was shown that for a certain EH system, there is an optimal value of time switching ratio which can minimize the system OP/SEP. Also, using multiple antennas at power beacon can greatly improve the performance of EH systems because of a significant increase about the amount of harvested energy. In addition, the non-linear characteristics of energy harvesters cause the power ceiling for the harvested energy leading to a error floor of OP/SEP in EH system [11]. Furthermore, EH technique is now combined with various new techniques such as full-duplex (FD), cognitive radio (CR), spatial modulation (SM), and non-orthogonal multiple access (NOMA) for enhancements in both energy and spectral efficiencies [7], [10]–[13]. In addition to the mathematical analysis, the experimental measurements were also used to investigate the amount of harvested energy and the performance of EH communication systems in practice [6], [14], [15].

On the other hand, the current wireless communication systems such as ZigBee, Long-term Evolution (LTE), WiFi, and Bluetooth are usually designed for short-range networks, where these systems can achieve reliable communications and high speed data transmissions [16]. However, the disadvantages of these systems are high energy consumption and high cost in deployment. Consequently, these systems cannot suitable for LoRa communications because of the low power consumption requirement of LoRa systems. In this context, low-power wide-area (LPWA) network technologies have been emerged as the promising connectivity solutions for IoT devices in recent years due to many advantages of LPWA systems [16], [17]. Particularly, LPWA technologies can reduce the power consumption with low delay sensitivity and wide coverage. Therefore, LPWA systems can solve various issues in the current wireless communication networks such as battery life, deployment cost, and coverage [16], [18]–[20]. The recent reports observed that, LPWA systems are highly promising for IoT requirements.

Beside the applications of LPWA systems for IoT devices, the performance of LPWA systems has been also investigated in the literature. In [19], a disruptive approach was proposed to increase the number of users used in LoRa systems. By applying

time-power multiplexing, the network capacity was significantly improved because the gateways can transmit more-than-one packets at the same time. Similarly [19], the works in [18] considered LoRA networks with an increase of IoT devices. The uplink OP was investigated over Poisson distributed channels when the interferences between IoT devices were taken into consideration. It was shown that the OP was greatly impacted by the interferences, distances, and the number of IoT devices. In [21], a theoretical analysis is conducted to investigate the feasibility of the transmission of a LoRa wide-area system via various conditions such as the effects of spreading factor (SF) and heights of transmit antennas. Their test results indicated that the system can transmit and receive at a far distance of 8.33 km. Together with the measured experiments, the mathematical analysis of LPWA systems was firstly performed in [22]. Specifically, [22] derived the OP and bit error rate (BER) expressions of LPWA system and validated them via computer simulations.

As the above discussions, both EH and LPWA network technologies have many advantages and can be applied for various applications in IoT systems. However, the combination of these two techniques have not been applied in the literature. In particular, the amount of harvested energy can fully satisfy the power requirements of IoT devices in LPWA systems. Therefore, exploiting EH technique for LPWA systems is inevitable in the future. This observation motivates us to considered an EH-LPWA system where IoT sensor can harvest the energy from power beacon and then use the harvested energy for transmitting signals. By using mathematical analysis, we obtain the exact closed-from expressions of OPs, throughputs, and SEPs of the considered EH-LPWA system. So far, this is the first work that mathematically analyzes the performance of LPWA system with EH technique. The main contributions of the paper are summarized as follows:

- We investigate an EH-LPWA system where EH technique is exploited. Specifically, IoT sensor is located in a restricted area, where the traditional power grid is extremely difficult to deploy. Thus, it has to harvest the energy from power beacon before transmitting signals to gateways. In addition, power beacon and gateways are equipped with multiple antennas.
- We derive the exact signal-to-noise (SNR) ratio at all gateways and server center, and then obtain the exact closed-form expressions of OPs, throughputs, and SEPs of the considered EH-LPWA system over Rayleigh fading channel for both cases without and with cooperative communications. We validate all derived expressions through Monte-Carlo simulations.
- We evaluate the performance of the considered EH-LPWA system for various scenarios. Particularly, the numerical results clarify that the data transmission rates, the distances, the time switching ratio for EH, and the number of transmit/receive antennas greatly impact on the OPs, throughputs, and SEPs of the system. By using a half of transmission block for EH, the system performance can be optimized. When the total of transmit and receive antennas are constant, we can use the number of transmit antennas at PB equal to the number of receive antennas at gateways to achieve the lowest OP/SEP of the considered EH-LPWA system.

The rest of this paper is organized as follows. Section II presents the system and signal model of the considered EH-LPWA system without and with cooperative communication. Section III analyzes the system performance by mathematically deriving the OP and SEP expressions for both cases without and with cooperative communication. Section IV provides numerical results and discussions. Finally, Section V concludes this paper.

II. System Model

The considered EH-LPWA system is illustrated in Fig. 1. The system consists of a power beacon (B), an IoT sensor (S), K gateways ($\mathrm{G}_1, \mathrm{G}_2$,..., G_K), and a server center (C). Specifically, S has only one antenna while B and G_k ($k = 1, 2, ..., K$), respectively, have M and N antennas. In addition, S is located in a restricted area, it is difficult to supply power to it. Therefore, S has to harvest the energy from B via radio frequency (RF) signals for data transmission. Since EH from RF signals can provide stable energy to IoT devices used in 5G and B5G networks [1], [6], the considered EH-LPWA system can be deployed in various applications including the traffic management, health care systems, environmental monitoring, and smart buildings [23]–[26].

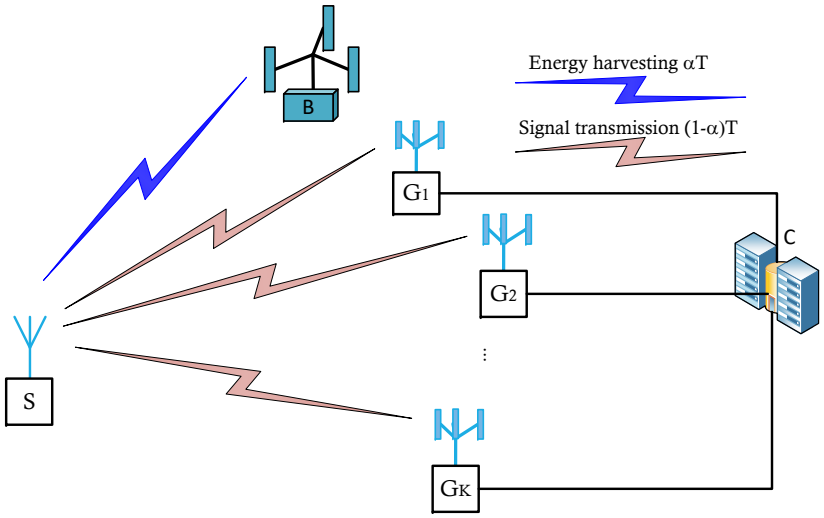

Fig. 1. Illustration of the considered EH-LPWA system.

There are two stages corresponding to time switching (TS) protocol for the system operation, as shown from Fig. 2. Firstly, S harvests the energy from B using the interval αT, where α is the time switching ratio satisfying $0 \leq \alpha \leq 1$ and T is the transmission block. Secondly, S transmits signals to all gateways using the remain interval $(1-\alpha)T$.

In the interval of EH, the harvested energy at S (denoted by E_{S}) is given as

$$E_{\mathrm{S}} = \frac{\eta \alpha T P_{\mathrm{B}} d_{\mathrm{BS}}^{-\beta} \|\mathbf{h}_{\mathrm{BS}}\|^2}{M}, \tag{1}$$

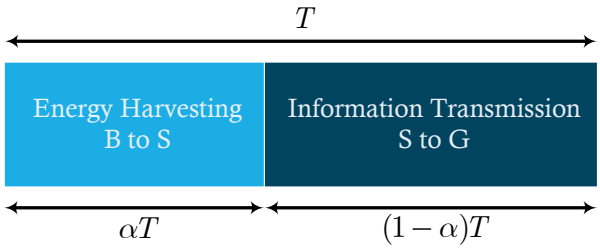

Fig. 2. TS protocol for the considered EH-LPWA system.

where η is the energy conversion efficiency ($0 \leq \eta \leq 1$); $P_{\rm B}$ is the total transmission power of B; $d_{\rm BS}$ is the distance between B and S; $2 \leq \beta \leq 6$ is the path-loss exponent; $\mathbf{h}_{\rm BS}$ is the channel vector from M transmit antennas of B to one receive antenna of S. Then, all the harvested energy at S is transformed to the power for signal transmission. The transmit power of S is thus given as

$$P_{\rm S} = \frac{E_{\rm S}}{(1-\alpha)T} = \frac{\eta\alpha T P_{\rm B} d_{\rm BS}^{-\beta} \|\mathbf{h}_{\rm BS}\|^2}{M(1-\alpha)T} = \frac{\eta\alpha P_{\rm B}\|\mathbf{h}_{\rm BS}\|^2}{M(1-\alpha)d_{\rm BS}^{\beta}}. \tag{2}$$

The received signals at G_k in the interval $(1-\alpha)T$ is computed as

$$y_{\mathrm{G}_k} = \mathbf{h}_{\mathrm{SG}_k}\sqrt{P_{\rm S} d_{\mathrm{SG}_k}^{-\beta}}x_{\rm S} + z_{\mathrm{G}_k}, \tag{3}$$

where $\mathbf{h}_{\mathrm{SG}_k}$ is the channel vector from one transmit antenna of S to N receive antennas of the kth gateway; $x_{\rm S}$ is the transmitted signal at S; d_{SG_k} is the distance from S to the kth gateway; z_{G_k} is the Gaussian noise at the kth gateway with zero mean and variance of σ^2, i.e., $z_{\mathrm{G}_k} \sim \mathcal{CN}(0, \sigma^2)$.

At the each gateway, maximum ratio combining (MRC) is applied to maximize the received signal power. Consequently, the signal-to-noise (SNR) ratio at the kth gateway is calculated as

$$\gamma_{\mathrm{G}_k} = \frac{\|\mathbf{h}_{\mathrm{SG}_k}\|^2 P_{\rm S} d_{\mathrm{SG}_k}^{-\beta}}{\sigma^2}. \tag{4}$$

In the case of cooperative communications, all the distances from S to all gateways are normalized for combining the signal at the server center [22]. Thus, the received signal at C is now expressed as

$$y_{\rm C} = \sqrt{P_{\rm S}\sum_{k=1}^{K}\|\mathbf{h}_{\mathrm{SG}_k}\|^2 d_0^{-\beta}}x_{\rm S} + z_{\rm C}, \tag{5}$$

where $d_0 = \min(d_{\mathrm{SG}_1}, d_{\mathrm{SG}_2}, ..., d_{\mathrm{SG}_K})$, and $z_{\rm C}$ is the Gaussian noise term.

From (5), the SNR at C is computed as

$$\gamma_{\rm C} = \frac{P_{\rm S}\sum\limits_{k=1}^{K}\|\mathbf{h}_{\mathrm{SG}_k}\|^2 d_0^{-\beta}}{\sigma^2}. \tag{6}$$

Replacing $P_{\rm S}$ from (2) into (4) and (6), the SNR at the kth gateway and C are, respectively, expressed as

$$\gamma_{{\rm G}_k} = \frac{\eta\alpha P_{\rm B}\|\mathbf{h}_{\rm BS}\|^2\|\mathbf{h}_{{\rm SG}_k}\|^2}{M\sigma^2(1-\alpha)d_{\rm BS}^{\beta}d_{{\rm SG}_k}^{\beta}}, \tag{7}$$

$$\gamma_{\rm C} = \frac{\eta\alpha P_{\rm B}\|\mathbf{h}_{\rm BS}\|^2\sum\limits_{k=1}^{K}\|\mathbf{h}_{{\rm SG}_k}\|^2}{M\sigma^2(1-\alpha)d_{\rm BS}^{\beta}d_0^{\beta}}. \tag{8}$$

III. Performance Analysis

A. Outage Probability

The OP of the considered EH-LPWA system is defined as the probability when the instantaneous data transmission rate is lower than the pre-defined data transmission rate. Mathematically, the OPs in the cases of without and with cooperative communication are, respectively, computed as

$$\mathcal{P}_k = \Pr\Big\{(1-\alpha)\log_2(1+\gamma_{{\rm G}_k}) < \mathcal{R}\Big\}, \tag{9}$$

$$\mathcal{P}_{\rm C} = \Pr\Big\{(1-\alpha)\log_2(1+\gamma_{\rm C}) < \mathcal{R}\Big\}, \tag{10}$$

where $\gamma_{{\rm G}_k}$ and $\gamma_{\rm C}$ are, respectively, given in (7) and (8); $\mathcal{R}$ is the pre-defined data transmission rate. It is better to note that, the pre-defined data transmission rate is calculated as the number of bits transmitted over the air per second via a bandwidth of 1 Hz. In other words, the pre-defined data transmission rate is also called as the spectral efficiency (bit/s/Hz) when the bandwidth is normalized as 1 Hz.

Let $\gamma_{\rm th} = 2^{\frac{\mathcal{R}}{1-\alpha}} - 1$ be the outage threshold, (9) and (10) can be rewritten as

$$\mathcal{P}_k = \Pr\Big\{\gamma_{{\rm G}_k} < \gamma_{\rm th}\Big\}, \tag{11}$$

$$\mathcal{P}_{\rm C} = \Pr\Big\{\gamma_{\rm C} < \gamma_{\rm th}\Big\}. \tag{12}$$

From (11) and (12), the OPs of the considered system are derived as the following Theorem 1.

Theorem 1: The OPs of the considered EH-LPWA system with energy harvesting in the cases without and with cooperative communications over Rayleigh fading channel are given as

$$\mathcal{P}_k = 1 - \frac{2}{\Gamma(N)}\sum_{m=0}^{M-1}\frac{1}{m!}\left(\frac{M\sigma^2(1-\alpha)d_{\rm BS}^{\beta}d_{{\rm SG}_k}^{\beta}\gamma_{\rm th}}{\eta\alpha P_{\rm B}}\right)^{\frac{N+m}{2}}\mathcal{K}_{N-m}\left(2\sqrt{\frac{M\sigma^2(1-\alpha)d_{\rm BS}^{\beta}d_{{\rm SG}_k}^{\beta}\gamma_{\rm th}}{\eta\alpha P_{\rm B}}}\right), \tag{13}$$

$$\mathcal{P}_{\rm C} = 1 - \frac{2}{\Gamma(KN)}\sum_{m=0}^{M-1}\frac{1}{m!}\left(\frac{M\sigma^2(1-\alpha)d_{\rm BS}^{\beta}d_0^{\beta}\gamma_{\rm th}}{\eta\alpha P_{\rm B}}\right)^{\frac{KN+m}{2}}\mathcal{K}_{KN-m}\left(2\sqrt{\frac{M\sigma^2(1-\alpha)d_{\rm BS}^{\beta}d_0^{\beta}\gamma_{\rm th}}{\eta\alpha P_{\rm B}}}\right), \tag{14}$$

where $\Gamma(.)$ is the gamma function; $\mathcal{K}_{N-m}(.)$ and $\mathcal{K}_{KN-m}(.)$ are the $N-m$ and $KN-m$ order modified Bessel functions of the second kind [27], respectively.

Proof: Replacing γ_{G_k} and γ_{C} in (7) and (8) into (11) and (12), respectively, the OPs are now expressed as

$$\begin{aligned}\mathcal{P}_k &= \Pr\left\{\frac{\eta\alpha P_{\mathrm{B}}\|\mathbf{h}_{\mathrm{BS}}\|^2\|\mathbf{h}_{\mathrm{SG}_k}\|^2}{M\sigma^2(1-\alpha)d_{\mathrm{BS}}^{\beta}d_{\mathrm{SG}_k}^{\beta}} < \gamma_{\mathrm{th}}\right\}\\ &= \Pr\left\{\|\mathbf{h}_{\mathrm{BS}}\|^2\|\mathbf{h}_{\mathrm{SG}_k}\|^2 < \frac{M\sigma^2(1-\alpha)d_{\mathrm{BS}}^{\beta}d_{\mathrm{SG}_k}^{\beta}\gamma_{\mathrm{th}}}{\eta\alpha P_{\mathrm{B}}}\right\}\\ &= 1-\int_0^{\infty}\left[1-F_{\|\mathbf{h}_{\mathrm{BS}}\|^2}\left(\frac{M\sigma^2(1-\alpha)d_{\mathrm{BS}}^{\beta}d_{\mathrm{SG}_k}^{\beta}\gamma_{\mathrm{th}}}{\eta\alpha P_{\mathrm{B}}y}\right)\right]f_{\|\mathbf{h}_{\mathrm{SG}_k}\|^2}(y)dy,\end{aligned} \tag{15}$$

$$\begin{aligned}\mathcal{P}_{\mathrm{C}} &= \Pr\left\{\frac{\eta\alpha P_{\mathrm{B}}\|\mathbf{h}_{\mathrm{BS}}\|^2\sum_{k=1}^{K}\|\mathbf{h}_{\mathrm{SG}_k}\|^2}{M\sigma^2(1-\alpha)d_{\mathrm{BS}}^{\beta}d_0^{\beta}} < \gamma_{\mathrm{th}}\right\}\\ &= \Pr\left\{\|\mathbf{h}_{\mathrm{BS}}\|^2\sum_{k=1}^{K}\|\mathbf{h}_{\mathrm{SG}_k}\|^2 < \frac{M\sigma^2(1-\alpha)d_{\mathrm{BS}}^{\beta}d_0^{\beta}\gamma_{\mathrm{th}}}{\eta\alpha P_{\mathrm{B}}}\right\}\\ &= 1-\int_0^{\infty}\left[1-F_{\|\mathbf{h}_{\mathrm{BS}}\|^2}\left(\frac{M\sigma^2(1-\alpha)d_{\mathrm{BS}}^{\beta}d_0^{\beta}\gamma_{\mathrm{th}}}{\eta\alpha P_{\mathrm{B}}z}\right)\right]f_{\sum_{k=1}^{K}\|\mathbf{h}_{\mathrm{SG}_k}\|^2}(z)dz,\end{aligned} \tag{16}$$

where $F(.)$ and $f(.)$ are respectively the cumulative distribution function (CDF) and the probability density function (PDF) of the instantaneous channel gain amplitude.

To derive the exact closed-form expressions from (15) and (16), we firstly obtain the CDF and PDF of the instantaneous channel gain following Rayleigh distribution. For only one channel gain, i.e., $|h|^2$, the CDF and PDF are, respectively, given as

$$F_{|h|^2}(x) = 1-\exp(-x),\ x \geq 0, \tag{17}$$

$$f_{|h|^2}(x) = \exp(-x),\ x \geq 0. \tag{18}$$

When maximal-ratio-transmission (MRT) and maximal-ratio-combining (MRC) techniques are applied at the transmitter/receiver, such as MRT at power beacon and MRC at kth gateway or server center, the CDF and PDF of channel gains, i.e, $\|\mathbf{h}_{\mathrm{BS}}\|^2$ are expressed as [28]:

$$F_{\|\mathbf{h}_{\mathrm{BS}}\|^2}(x) = 1-\exp(-x)\sum_{m=0}^{M-1}\frac{x^m}{m!},\quad x \geq 0, \tag{19}$$

$$f_{\|\mathbf{h}_{\mathrm{BS}}\|^2}(x) = \frac{x^{M-1}\exp(-x)}{\Gamma(M)},\quad x \geq 0. \tag{20}$$

Now, applying (19) and (20), the probabilities in (15) and (16) are solved as

$$\begin{aligned}\mathcal{P}_k &= 1 - \int_0^\infty \exp\left(- \frac{M\sigma^2(1-\alpha)d_{\rm BS}^\beta d_{{\rm SG}_k}^\beta \gamma_{\rm th}}{\eta\alpha P_{\rm B} y}\right) \sum_{m=0}^{M-1} \frac{1}{m!}\left(\frac{M\sigma^2(1-\alpha)d_{\rm BS}^\beta d_{{\rm SG}_k}^\beta \gamma_{\rm th}}{\eta\alpha P_{\rm B} y}\right)^m \frac{y^{N-1}\exp(-y)}{\Gamma(N)} dy \\ &= 1 - \frac{1}{\Gamma(N)} \sum_{m=0}^{M-1} \frac{1}{m!}\left(\frac{M\sigma^2(1-\alpha)d_{\rm BS}^\beta d_{{\rm SG}_k}^\beta \gamma_{\rm th}}{\eta\alpha P_{\rm B}}\right)^m \int_0^\infty \exp\left(- \frac{M\sigma^2(1-\alpha)d_{\rm BS}^\beta d_{{\rm SG}_k}^\beta \gamma_{\rm th}}{\eta\alpha P_{\rm B} y} - y\right) y^{N-m-1} dy, \end{aligned} \tag{21}$$

$$\begin{aligned}\mathcal{P}_{\rm C} &= 1 - \int_0^\infty \exp\left(- \frac{M\sigma^2(1-\alpha)d_{\rm BS}^\beta d_0^\beta \gamma_{\rm th}}{\eta\alpha P_{\rm B} z}\right) \sum_{m=0}^{M-1} \frac{1}{m!}\left(\frac{M\sigma^2(1-\alpha)d_{\rm BS}^\beta d_0^\beta \gamma_{\rm th}}{\eta\alpha P_{\rm B} z}\right)^m \frac{z^{KN-1}\exp(-z)}{\Gamma(KN)} dz \\ &= 1 - \frac{1}{\Gamma(KN)} \sum_{m=0}^{M-1} \frac{1}{m!}\left(\frac{M\sigma^2(1-\alpha)d_{\rm BS}^\beta d_0^\beta \gamma_{\rm th}}{\eta\alpha P_{\rm B}}\right)^m \int_0^\infty \exp\left(- \frac{M\sigma^2(1-\alpha)d_{\rm BS}^\beta d_0^\beta \gamma_{\rm th}}{\eta\alpha P_{\rm B} z} - z\right) z^{KN-m-1} dz. \end{aligned} \tag{22}$$

Applying [27, Eq. (3.471.9)], two above integrals are computed as

$$\begin{aligned}&\int_0^\infty \exp\left(- \frac{M\sigma^2(1-\alpha)d_{\rm BS}^\beta d_{{\rm SG}_k}^\beta \gamma_{\rm th}}{\eta\alpha P_{\rm B} y} - y\right) y^{N-m-1} dy \\ &= 2\left(\frac{M\sigma^2(1-\alpha)d_{\rm BS}^\beta d_{{\rm SG}_k}^\beta \gamma_{\rm th}}{\eta\alpha P_{\rm B}}\right)^{\frac{N-m}{2}} \mathcal{K}_{N-m}\left(2\sqrt{\frac{M\sigma^2(1-\alpha)d_{\rm BS}^\beta d_{{\rm SG}_k}^\beta \gamma_{\rm th}}{\eta\alpha P_{\rm B}}}\right), \end{aligned} \tag{23}$$

$$\begin{aligned}&\int_0^\infty \exp\left(- \frac{M\sigma^2(1-\alpha)d_{\rm BS}^\beta d_0^\beta \gamma_{\rm th}}{\eta\alpha P_{\rm B} z} - z\right) z^{KN-m-1} dz \\ &= 2\left(\frac{M\sigma^2(1-\alpha)d_{\rm BS}^\beta d_0^\beta \gamma_{\rm th}}{\eta\alpha P_{\rm B}}\right)^{\frac{KN-m}{2}} \mathcal{K}_{KN-m}\left(2\sqrt{\frac{M\sigma^2(1-\alpha)d_{\rm BS}^\beta d_0^\beta \gamma_{\rm th}}{\eta\alpha P_{\rm B}}}\right). \end{aligned} \tag{24}$$

Replacing (23) and (24) into (21) and (22), respectively, we obtain the exact closed-form expressions of OPs of the considered EH-LPWA system as in Theorem 1. Hence, the proof is completed.

B. Symbol Error Probability

The SEP of the considered EH-LPWA system is expressed as

$$\text{SEP} = a\mathbb{E}\{Q(\sqrt{b\gamma})\} = \frac{a}{\sqrt{2\pi}} \int_0^\infty F\Big(\frac{t^2}{b}\Big) e^{-\frac{t^2}{2}} dt, \tag{25}$$

where (a, b) is a couple of the modulation types, i.e., $(a, b) = (1, 2)$ and $(a, b) = (2, 1)$ for the binary phase-shift keying (BPSK) and 4-quadrature amplitude modulation (4-QAM), respectively [29]. Other values of (a, b) are given as in Table 6.1 of [29]; $Q(.)$ denotes the Gaussian function; γ is SNR of the considered system, which is given as (7) and (8) for the cases without and with cooperative communication, respectively. By changing the variable, i.e., $x = \frac{t^2}{b}$, (25) can be rewritten as

$$\text{SEP} = \frac{a\sqrt{b}}{2\sqrt{2\pi}} \int_0^\infty \frac{F(x)}{\sqrt{x}} \exp\Big(- \frac{bx}{2}\Big) dx. \tag{26}$$

Based on (26), the SEPs of the considered EH-LPWA system are derived in the following Theorem 2.

Theorem 2: The SEPs of the considered EH-LPWA system with energy harvesting in the cases without and with cooperative communication over Rayleigh fading channel are, respectively, given as

$$\begin{aligned}\mathrm{SEP}_k =&\frac{a\sqrt{b}}{2\sqrt{2\pi}}\Bigg[\sqrt{\frac{2\pi}{b}}-\frac{1}{\Gamma(N)}\Gamma\Big(N+\frac{1}{2}\Big)\exp\left(\frac{M\sigma^2(1-\alpha)d_{\mathrm{BS}}^{\beta}d_{\mathrm{SG}_k}^{\beta}}{b\eta\alpha P_{\mathrm{B}}}\right)\\&\times\sum_{m=0}^{M-1}\frac{\Gamma\Big(m+\frac{1}{2}\Big)}{m!}\Big(\frac{b}{2}\Big)^{-\frac{N+m}{2}}\left(\frac{M\sigma^2(1-\alpha)d_{\mathrm{BS}}^{\beta}d_{\mathrm{SG}_k}^{\beta}}{\eta\alpha P_{\mathrm{B}}}\right)^{\frac{N+m-1}{2}}\mathcal{W}_{-\frac{N+m}{2},\frac{N-m}{2}}\left(\frac{2M\sigma^2(1-\alpha)d_{\mathrm{BS}}^{\beta}d_{\mathrm{SG}_k}^{\beta}}{b\eta\alpha P_{\mathrm{B}}}\right)\Bigg],\end{aligned}\tag{27}$$

$$\begin{aligned}\mathrm{SEP}_{\mathrm{C}} =&\frac{a\sqrt{b}}{2\sqrt{2\pi}}\Bigg[\sqrt{\frac{2\pi}{b}}-\frac{1}{\Gamma(KN)}\Gamma\Big(KN+\frac{1}{2}\Big)\exp\left(\frac{M\sigma^2(1-\alpha)d_{\mathrm{BS}}^{\beta}d_{0}^{\beta}}{b\eta\alpha P_{\mathrm{B}}}\right)\\&\times\sum_{m=0}^{M-1}\frac{\Gamma\Big(m+\frac{1}{2}\Big)}{m!}\Big(\frac{b}{2}\Big)^{-\frac{KN+m}{2}}\left(\frac{M\sigma^2(1-\alpha)d_{\mathrm{BS}}^{\beta}d_{0}^{\beta}}{\eta\alpha P_{\mathrm{B}}}\right)^{\frac{KN+m-1}{2}}\mathcal{W}_{-\frac{KN+m}{2},\frac{KN-m}{2}}\left(\frac{2M\sigma^2(1-\alpha)d_{\mathrm{BS}}^{\beta}d_{0}^{\beta}}{b\eta\alpha P_{\mathrm{B}}}\right)\Bigg],\end{aligned}\tag{28}$$

where $\mathcal{W}_{.,.}(.)$ is the Whittaker functions [27].

Proof: To obtain the SEPs of the considered EH-LPWA system, firstly, we derive the CDF, $F(x)$ in the cases of non-cooperative and cooperative communications. Based on the definition of $F(x)$, i.e.,

$$F(x)=\Pr\{\gamma<x\},\tag{29}$$

we can easily obtain the CDFs of the considered EH-LPWA system in the cases of non-cooperative and cooperative communications by replacing γ_{th} by x in the OP expressions. Therefore, the CDFs in the cases of non-cooperative ($F_k(x)$) and cooperative ($F_{\mathrm{C}}(x)$) communications are derived as

$$F_k(x)=1-\frac{2}{\Gamma(N)}\sum_{m=0}^{M-1}\frac{1}{m!}\left(\frac{M\sigma^2(1-\alpha)d_{\mathrm{BS}}^{\beta}d_{\mathrm{SG}_k}^{\beta}x}{\eta\alpha P_{\mathrm{B}}}\right)^{\frac{N+m}{2}}\mathcal{K}_{N-m}\left(2\sqrt{\frac{M\sigma^2(1-\alpha)d_{\mathrm{BS}}^{\beta}d_{\mathrm{SG}_k}^{\beta}x}{\eta\alpha P_{\mathrm{B}}}}\right),\tag{30}$$

$$F_{\mathrm{C}}(x)=1-\frac{2}{\Gamma(KN)}\sum_{m=0}^{M-1}\frac{1}{m!}\left(\frac{M\sigma^2(1-\alpha)d_{\mathrm{BS}}^{\beta}d_{0}^{\beta}x}{\eta\alpha P_{\mathrm{B}}}\right)^{\frac{KN+m}{2}}\mathcal{K}_{KN-m}\left(2\sqrt{\frac{M\sigma^2(1-\alpha)d_{\mathrm{BS}}^{\beta}d_{0}^{\beta}x}{\eta\alpha P_{\mathrm{B}}}}\right).\tag{31}$$

Replacing (30) and (31), the SEPs are now expressed as

$$\begin{aligned}\mathrm{SEP}_k =&\frac{a\sqrt{b}}{2\sqrt{2\pi}}\int_0^{\infty}\frac{\exp\Big(-\frac{bx}{2}\Big)}{\sqrt{x}}\left[1-\frac{2}{\Gamma(N)}\sum_{m=0}^{M-1}\frac{1}{m!}\left(\frac{M\sigma^2(1-\alpha)d_{\mathrm{BS}}^{\beta}d_{\mathrm{SG}_k}^{\beta}x}{\eta\alpha P_{\mathrm{B}}}\right)^{\frac{N+m}{2}}\mathcal{K}_{N-m}\left(2\sqrt{\frac{M\sigma^2(1-\alpha)d_{\mathrm{BS}}^{\beta}d_{\mathrm{SG}_k}^{\beta}x}{\eta\alpha P_{\mathrm{B}}}}\right)\right]dx\\=&\frac{a\sqrt{b}}{2\sqrt{2\pi}}\Bigg[\int_0^{\infty}\frac{\exp\Big(-\frac{bx}{2}\Big)}{\sqrt{x}}dx-\frac{2}{\Gamma(N)}\sum_{m=0}^{M-1}\frac{1}{m!}\left(\frac{M\sigma^2(1-\alpha)d_{\mathrm{BS}}^{\beta}d_{\mathrm{SG}_k}^{\beta}}{\eta\alpha P_{\mathrm{B}}}\right)^{\frac{N+m}{2}}\\&\times\int_0^{\infty}x^{\frac{N+m-1}{2}}\exp\Big(-\frac{bx}{2}\Big)\mathcal{K}_{N-m}\left(2\sqrt{\frac{M\sigma^2(1-\alpha)d_{\mathrm{BS}}^{\beta}d_{\mathrm{SG}_k}^{\beta}x}{\eta\alpha P_{\mathrm{B}}}}\right)dx\Bigg].\end{aligned}\tag{32}$$

$$\begin{aligned}\mathrm{SEP_C} =&\frac{a\sqrt{b}}{2\sqrt{2\pi}}\int_0^\infty \frac{\exp\left(-\frac{bx}{2}\right)}{\sqrt{x}}\left[1-\frac{2}{\Gamma(KN)}\sum_{m=0}^{M-1}\frac{1}{m!}\left(\frac{M\sigma^2(1-\alpha)d_{\mathrm{BS}}^{\beta}d_0^{\beta}x}{\eta\alpha P_{\mathrm{B}}}\right)^{\frac{KN+m}{2}}\mathcal{K}_{KN-m}\left(2\sqrt{\frac{M\sigma^2(1-\alpha)d_{\mathrm{BS}}^{\beta}d_0^{\beta}x}{\eta\alpha P_{\mathrm{B}}}}\right)\right]dx\\ =&\frac{a\sqrt{b}}{2\sqrt{2\pi}}\left[\int_0^\infty \frac{\exp\left(-\frac{bx}{2}\right)}{\sqrt{x}}dx-\frac{2}{\Gamma(KN)}\sum_{m=0}^{M-1}\frac{1}{m!}\left(\frac{M\sigma^2(1-\alpha)d_{\mathrm{BS}}^{\beta}d_0^{\beta}}{\eta\alpha P_{\mathrm{B}}}\right)^{\frac{KN+m}{2}}\right.\\ &\left.\times\int_0^\infty x^{\frac{KN+m-1}{2}}\exp\left(-\frac{bx}{2}\right)\mathcal{K}_{KN-m}\left(2\sqrt{\frac{M\sigma^2(1-\alpha)d_{\mathrm{BS}}^{\beta}d_0^{\beta}x}{\eta\alpha P_{\mathrm{B}}}}\right)dx\right].\end{aligned} \tag{33}$$

Applying [27, Eq. (6.643.3)], two integrals in (32) and (33) are now calculated as

$$\begin{aligned}&\int_0^\infty x^{\frac{N+m-1}{2}}\exp\left(-\frac{bx}{2}\right)\mathcal{K}_{N-m}\left(2\sqrt{\frac{M\sigma^2(1-\alpha)d_{\mathrm{BS}}^{\beta}d_{\mathrm{SG}_k}^{\beta}x}{\eta\alpha P_{\mathrm{B}}}}\right)dx\\ &=\Gamma\left(N+\frac{1}{2}\right)\Gamma\left(m+\frac{1}{2}\right)\exp\left(\frac{M\sigma^2(1-\alpha)d_{\mathrm{BS}}^{\beta}d_{\mathrm{SG}_k}^{\beta}}{b\eta\alpha P_{\mathrm{B}}}\right)\left(\frac{b}{2}\right)^{-\frac{N+m}{2}}\\ &\times\frac{1}{2\sqrt{\frac{M\sigma^2(1-\alpha)d_{\mathrm{BS}}^{\beta}d_{\mathrm{SG}_k}^{\beta}}{\eta\alpha P_{\mathrm{B}}}}}\mathcal{W}_{-\frac{N+m}{2},\frac{N-m}{2}}\left(\frac{2M\sigma^2(1-\alpha)d_{\mathrm{BS}}^{\beta}d_{\mathrm{SG}_k}^{\beta}}{b\eta\alpha P_{\mathrm{B}}}\right),\end{aligned} \tag{34}$$

$$\begin{aligned}&\int_0^\infty x^{\frac{KN+m-1}{2}}\exp\left(-\frac{bx}{2}\right)\mathcal{K}_{KN-m}\left(2\sqrt{\frac{M\sigma^2(1-\alpha)d_{\mathrm{BS}}^{\beta}d_0^{\beta}x}{\eta\alpha P_{\mathrm{B}}}}\right)dx\\ &=\Gamma\left(KN+\frac{1}{2}\right)\Gamma\left(m+\frac{1}{2}\right)\exp\left(\frac{M\sigma^2(1-\alpha)d_{\mathrm{BS}}^{\beta}d_0^{\beta}}{b\eta\alpha P_{\mathrm{B}}}\right)\left(\frac{b}{2}\right)^{-\frac{KN+m}{2}}\\ &\times\frac{1}{2\sqrt{\frac{M\sigma^2(1-\alpha)d_{\mathrm{BS}}^{\beta}d_0^{\beta}}{\eta\alpha P_{\mathrm{B}}}}}\mathcal{W}_{-\frac{KN+m}{2},\frac{KN-m}{2}}\left(\frac{2M\sigma^2(1-\alpha)d_{\mathrm{BS}}^{\beta}d_0^{\beta}}{b\eta\alpha P_{\mathrm{B}}}\right).\end{aligned} \tag{35}$$

Replacing (34) and (35) into (32) and (33), we obtain the SEPs of the considered system as in the Theorem 2. The proof is thus completed.

IV. Numerical Results and Discussions

In this section, the performance of the considered EH-LPWA system is evaluated via mathematical expressions in the previous section. To demonstrate the correctness of our derived expressions, the Monte-Carlo simulations are also provided in all investigated scenarios using 10^7 channel realizations. In all scenarios, the average SNR is calculated as the ratio between the average transmit power of power beacon and the noise power, i.e., SNR = P_{B}/σ^2. Additionally, the energy harvesting efficiency is chosen as $\eta = 0.85$[1]. Other parameters are varied to investigate their impacts on the OPs and SEPs of the considered EH-LPWA system. To clarify, the simulation parameters are listed in Tab. I.

Fig. 3 illustrates the OPs of the considered EH-LPWA system versus the average SNR with four gateways ($K = 4$). The transmit and receive antennas at B and G are chosen as $M = N = 3$. The distances are $d_{\mathrm{BS}} = 1$, $d_{\mathrm{SG}_1} = 2$, $d_{\mathrm{SG}_2} = 3$, $d_{\mathrm{SG}_3} = 4$,

[1]In practice, the energy harvesting efficiency η depends on the rectification process and the energy harvesting circuitry. The measurements and experiments demonstrated that, it ranges from 0.13 to 0.95 [30]. Therefore, it is often selected as 0.5 [5], [31], 0.8 [9], or 1 [6]. Thus, the assumption $\eta = 0.85$ in this paper is still valid for consideration. However, it may be lower than 0.85 in practical scenarios.

TABLE I

SIMULATION PARAMETERS FOR EVALUATING THE SYSTEM PERFORMANCE.

Notation	Description	Fixed value	Varying range
SNR	Signal-to-noise ratio	30 dB	20, 25 dB; $0 \sim 40$ dB
σ^2	Variance of Gaussian noise	1	none
η	Energy harvesting efficiency	0.85	none
α	Time switching ratio	0.5	$0.1 \sim 0.9$
d_{BS}	Distance between B and S	1	none
d_{SG_k}	Distance from S to the kth gateway	2	3, 4, 5
β	Path-loss exponent	3	2
K	Number of gateways	4	2
M	Number of transmit antennas at B	3	2, 4
N	Number of receive antennas at kth gateway	3	2, 4
$\mathcal{R}$	Pre-defined data transmission rate	1.5 bit/s/Hz	1, 2, 3 bit/s/Hz
(a, b)	A couple of the modulation types	$(2, 1)$	$(3, 1/5)$

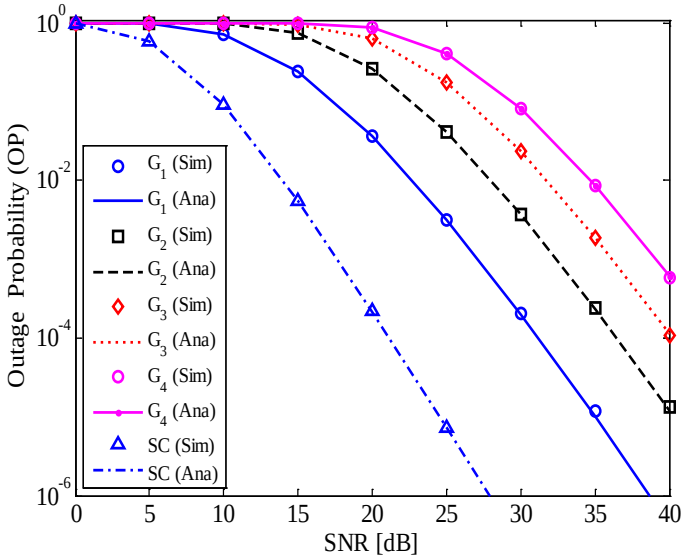

Fig. 3. The OPs of the considered EH-LPWA system versus the average SNR for $K = 4$, $M = N = 3$, $d_{\mathrm{BS}} = 1$, $d_{\mathrm{SG}_1} = 2$, $d_{\mathrm{SG}_2} = 3$, $d_{\mathrm{SG}_3} = 4$, $d_{\mathrm{SG}_4} = 5$, $\beta = 3$, $\alpha = 0.5$, $\mathcal{R} = 1.5$ bit/s/Hz.

$d_{\mathrm{SG}_4} = 5$, and the path loss exponent is $\beta = 3$. The time switching ratio is $\alpha = 0.5$[2]. The predefined data transmission rate

[2]It is noteworthy that the system parameters are chosen by measurements and experiments in practice. Specifically, the distances are often nominalized [32] or selected from 1 to 3 [11]. The path loss exponent ranges from 2 to 6, thus, many works chose it as $\beta = 2.5$ [9], $\beta = 2.7$ [11], [32], and $\beta = 3$ [22]. For half-duplex transmission, the time switching ratio α is often chosen from 0.3 to 0.5 because this range can minimize the OP (or SEP) and maximize the throughput of the half-duplex wireless systems [32], [33]. Similar to the measurements and experiments reported in previous works [5], [6], [11], [22], [31], [32], in this paper, we use $\beta = 2$ or 3, $\alpha = 0.5$ and $\eta = 0.85$ for the system evaluations. On the other hand, we also change the value of α from 0.1 to 0.9 to determine its impact on the OP of the considered EH-LPWA system.

is $\mathcal{R} = 1.5$ bit/s/Hz [3]. The analysis curves in Fig. 3 are plotted by using (13) and (14) corresponding to the OPs at gateways (denoted by G_1, G_2, G_3, and G_4) and server center (denoted by SC), respectively. Meanwhile, the markers denote the simulation results. It is obvious from Fig. 3, the distances greatly impact on the OPs of the considered EH-LPWA system because the OP of G_1 significantly lower than that of G_4. Also, the cooperative communication can remarkably improve the performance of the considered EH-LPWA system. Specifically, when the OP requirement is 10^{-3}, the case of cooperative communication only needs SNR = 17 dB, meanwhile, G_1, G_2, G_3, and G_4 need 27, 32, 35, and 38 dB, respectively, to satisfy this requirement. Since the received signal power at the server center is significantly enhanced with cooperative communication, the performance in the case with cooperative communication is much better than that in the case without cooperative communication. In other words, γ_{C} given in (8) is greatly higher than γ_{G_k} given in (7), the OP with cooperative communication is significantly lower than those without cooperative communication.

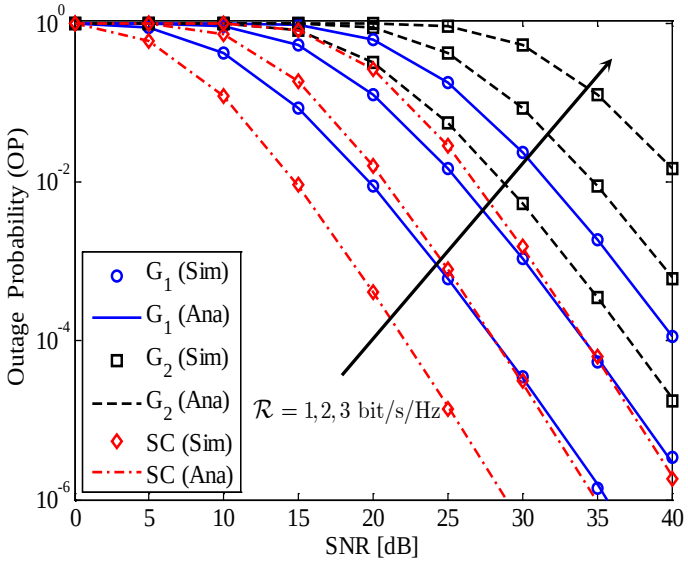

Fig. 4. The impact of data transmission rates on the OPs of the considered EH-LPWA system, for $K = 2$, $M = N = 3$, $d_{\mathrm{BS}} = 1$, $d_{\mathrm{SG}_1} = 2$, $d_{\mathrm{SG}_2} = 4$, $\beta = 3$, $\alpha = 0.5$, $\mathcal{R} = 1, 2, 3$ bit/s/Hz.

Fig. 4 presents the impact of data transmission rates on the OPs of the EH-LPWA system for $\mathcal{R} = 1, 2, 3$ bit/s/Hz. For easy observation, we choose $K = 2$ gateways. It can be seen that the high OPs can be achieved with high data transmission rates. In other words, the usage of high data transmission rates greatly reduces the performance of the considered EH-LPWA system. Particularly, at SNR = 40 dB, the OP at G_2 is only 10^{-2} for $\mathcal{R} = 3$ bit/s/Hz while it is nearly 10^{-5} for $\mathcal{R} = 1$ bit/s/Hz. On the other hand, the OPs at G_1 in the cases of $\mathcal{R} = 1$ bit/s/Hz and $\mathcal{R} = 2$ bit/s/Hz are similar with the OPs at

[3]Note that the predefined data transmission rates are corresponding to the modulation types and the bandwidth. For example, $\mathcal{R} = 1.5$ bit/s/Hz is equivalent to transmit 3 bits (8-QAM) per second via a bandwidth of 2 Hz. Similarly, $\mathcal{R} = 1, 2$, and 3 bit/s/Hz are equivalent to transmit 1, 2, and 3 bits (corresponding to BPSK, 4-QAM, and 8-QAM) per second via a bandwidth of 1 Hz.

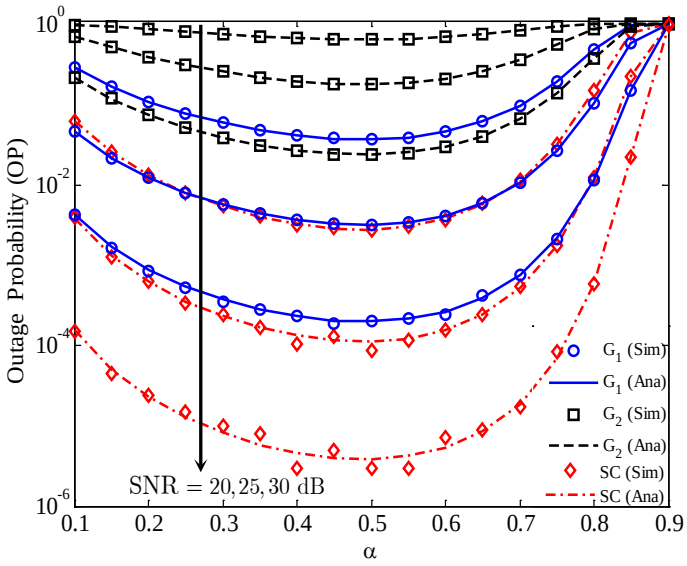

Fig. 5. The OPs of the considered EH-LPWA system versus the time switching ratio α for different SNRs, $K = 2$, $M = N = 3$, $d_{\mathrm{BS}} = 1$, $d_{\mathrm{SG}_1} = 2$, $d_{\mathrm{SG}_2} = 4$, $\beta = 3$, $\mathcal{R} = 1.5$ bit/s/Hz.

server center in the cases of $\mathcal{R} = 2$ bit/s/Hz and $\mathcal{R} = 3$ bit/s/Hz, respectively. Therefore, depending on the requirements of the considered EH-LPWA system in practice, we can choose the cases with or without cooperative communications corresponding to the suitable data transmission rate to reduce the signal processing complexity. For example, when SNR is fixed at SNR = 25 dB and the OP is required as 10^{-3}, we can either use one gateway (G_1) and choose $\mathcal{R} = 1$ bit/s/Hz to avoid the signal processing complexity at server center or use the cooperative communication with two gateways and higher data transmission rate ($\mathcal{R} = 2$ bit/s/Hz).

Fig. 5 determines the impact of the time switching ratio α on the OPs of the considered EH-LPWA system for different SNRs, i.e., SNR = 20, 25, 30 dB. As observed from Fig. 5, the OPs are minimum when $\alpha = 0.5$. In other word, the usage a half of one transmission block for EH is optimal for the considered EH-LPWA system. It is reasonable because the performance of the system depends on both α and transmit power of sensor. When α is low, that means the time duration for EH is low and the time duration for signal transmission is high, leading to the transmit power of sensor is also low. Thus, the OP performance is low. When α is higher, the time duration is higher for EH but lower for signal transmission. Consequently, the transmit power of sensor is higher but it is difficult to detect successfully received signals at the gateways because of lower time duration for signal transmission. On the other hand, in the case of we cannot use the optimal value of α ($\alpha = 0.5$), we can use $\alpha < 0.5$ to achieve better performance of the considered EH-LPWA system. It is because the OPs with $\alpha = 0.2, 0.4$ are lower than those with $\alpha = 0.8, 0.6$, respectively. It is better to note that, although the optimal problems were not presented in our analysis, however, by using obtained expressions, i.e., the OP expressions given in (13) and (14), we can figure out an

optimal α for improving the performance of the considered EH-LPWA system. As the results, depending on a specific value of the transmission power of the power beacon in practice, we can choose a suitable value of time switching ratio α to achieve the better performance of the considered EH-LPWA system.

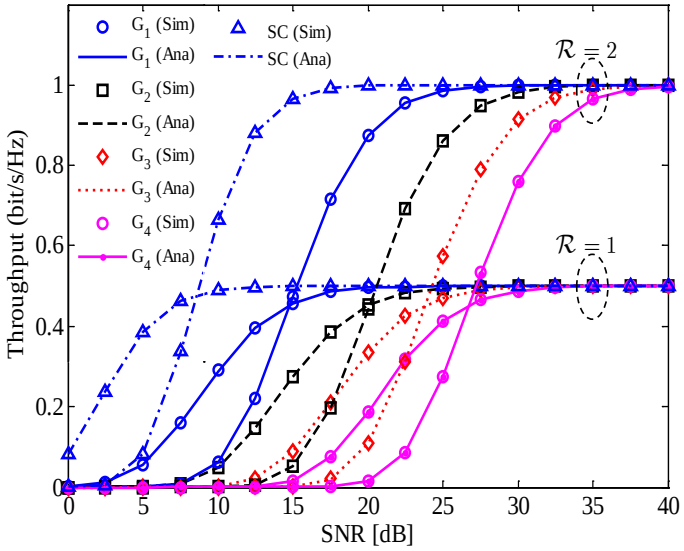

Fig. 6. The throughput of the considered EH-LPWA system versus the average SNR for two data transmission rates, $K = 4$, $M = N = 3$, $d_{\rm BS} = 1$, $d_{{\rm SG}_1} = 2$, $d_{{\rm SG}_2} = 3$, $d_{{\rm SG}_3} = 4$, $d_{{\rm SG}_4} = 5$, $\beta = 3$, $\alpha = 0.5$, $\mathcal{R} = 1, 2$ bit/s/Hz.

In Fig. 6, we evaluate the throughput of the considered EH-LPWA system, where the throughput is computed as $\mathcal{T} = \mathcal{R}(1-\alpha)(1-\mathcal{P})$, herein, $\mathcal{P}$ is given as (13) and (14) for the case of without and with cooperative communication, respectively. Since $\alpha = 0.5$, there is only a half of transmission block for transmitting signals, thus, the throughput is reduced a half in comparison with the case without energy harvesting. It can be seen from this figure, in the case of low data transmission rate, i.e., $\mathcal{R} = 1$ bit/s/Hz, all gateways and server center can get a half of the target throughput at SNR $>$ 30 dB. However, with higher data transmission rate, i.e., $\mathcal{R} = 2$ bit/s/Hz, it needs SNR = 38 dB to achieve a half of the target throughput for all gateways and server center. On the other hand, the differences between the throughput of all gateways are significant in low SNR regime, especially for $\mathcal{R} = 2$ bit/s/Hz. An other observation from Figs. 3–6 is that the data transmission rates can be chosen higher, i.e., $\mathcal{R} = 4, 5, ...$ bit/s/Hz. Although higher $\mathcal{R}$ will reduce the OP and throughput performance of the considered EH-LPWA system, the features of the OP and throughput curves are still similar to those in the case of $\mathcal{R} = 1, 2$, and 3 bit/s/Hz. Thus, we often use $\mathcal{R} = 1, 2$, and 3 bit/s/Hz in most figures for easy observation.

The SEPs of the considered EH-LPWA system versus the average SNR for two modulation schemes, i.e., 4QAM ($a = 2, b = 1$) and 16QAM ($a = 3, b = 1/5$), are illustrated in Fig. 7. We use (27) and (28) to plot the analysis curves of SEPs in the case without and with the cooperative communication, respectively. Similar to the OPs, with the higher order modulation scheme,

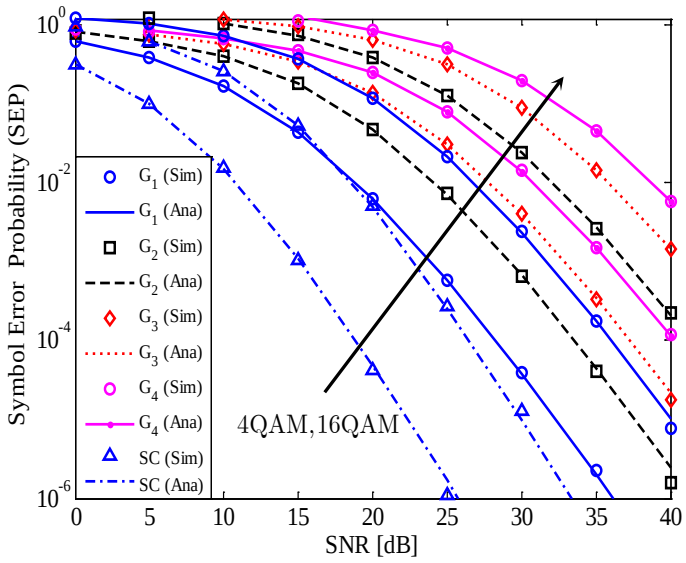

Fig. 7. The SEPs of the considered EH-LPWA system versus the average SNR for two modulation schemes, $K = 4$, $M = N = 3$, $d_{\mathrm{BS}} = 1$, $d_{\mathrm{SG}_1} = 2$, $d_{\mathrm{SG}_2} = 3$, $d_{\mathrm{SG}_3} = 4$, $d_{\mathrm{SG}_4} = 5$, $\beta = 3$, $\alpha = 0.5$.

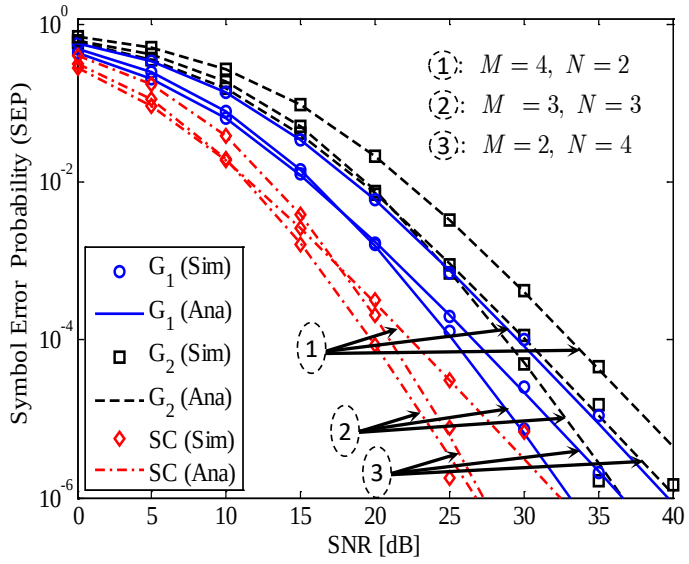

Fig. 8. The impacts of number of transmit antennas at power beacon and number of received antennas at gateways on the SEPs of the considered EH-LPWA system, $K = 2$, $d_{\mathrm{BS}} = 1$, $d_{\mathrm{SG}_1} = 2$, $d_{\mathrm{SG}_2} = 3$, $\beta = 2$, $\alpha = 0.5$.

the higher SEPs can be achieved. In particular, the diversity order of the G_1, G_2, and the cooperative communication system is three, which is equal to the number of receive antennas at G_1 and G_2. Meanwhile, the diversity order of the G_3 and G_4 is two, it is less than the number of receive antennas at G_3 and G_4. These results are reasonable, because the distances from sensor to G_1 and G_2 are less than these from sensor to G_3 and G_4 ($d_{\mathrm{SG}_1} = 2$, $d_{\mathrm{SG}_2} = 3$, $d_{\mathrm{SG}_3} = 4$, $d_{\mathrm{SG}_4} = 5$).

Fig. 8 investigates the impacts of the number of transmit antennas at power beacon and the number of receive antennas at gateways on the SEPs of the considered EH-LPWA system with $M + N = 6$, using 4-QAM. As shown from Fig. 8, the case

of $M = N = 3$ (circle two in this figure) is the best case and the case of $M = 4, N = 2$ (circle one in this figure) is the worst case among three considered cases. These results are reasonable for the considered EH-LPWA system. It is because the performance of the considered system is improved when the SNRs at the kth gateway and server center increase. Meanwhile, these SNRs depend on the transmit power of IoT sensor ($P_{\rm S}$) and ${\rm SG}_k$ channel gains ($\|\mathbf{h}_{{\rm SG}_k}\|^2$). When M increases, the harvested energy at S will increase leading to $P_{\rm S}$ increases. Similarly, when N increases, the received signal power at the gateways will be increased because $\|\mathbf{h}_{{\rm SG}_k}\|^2$ increases. As the results, when $M + N$ is a constant, we need to find the certain values of M and N to achieve the best performance of the considered system. In that context, the case of $M = N = 3$ is the best case in among three investigated cases because this the case can balance both $P_{\rm S}$ and $\|\mathbf{h}_{{\rm SG}_k}\|^2$. In other words, in the case of $M = 4, N = 2$, $P_{\rm S}$ increases but $\|\mathbf{h}_{{\rm SG}_k}\|^2$ significantly decreases in comparison with the case of $M = N = 3$, thus, the performance in the case of $M = 4, N = 2$ is lower than that of $M = N = 3$. Similarly, in the case of $M = 2, N = 4$, although $\|\mathbf{h}_{{\rm SG}_k}\|^2$ increases but $P_{\rm S}$ greatly reduces in comparison with the case of $M = N = 3$, thus, the performance in the case of $M = 2, N = 4$ is also lower than that of $M = N = 3$. From this observation, we can use the number of transmit antennas at power beacon equal to the number of receive antennas at gateways to achieve the best performance of the considered EH-LPWA system.

V. Conclusion

Applying energy harvesting for sensor in IoT systems is inevitable for future wireless networks, especially for low-power wide-are systems. Therefore, in this paper, we exploit EH for LPWA system and mathematically analyze the performance of the EH-LPWA system by deriving the exact closed-form expressions of outage probability, throughput, and symbol error probability to clearly show the system behaviors for both cases without and with cooperative communications. Numerical results have confirmed that the distances and the data transmission rates have great impacts on the OPs, throughputs, and SEPs of the considered EH-LPWA system. Specifically, the usage of a half of time duration of transmission block for energy harvesting can achieve the best performance for the EH-LPWA system. Also, due to the time duration for energy harvesting, the considered EH-LPWA system throughput cannot reach the target throughput. In addition, the diversity order of the considered EH-LPWA system in the case without cooperative communication can be equal to the number of receive antennas at the gateways for a certain distances. Furthermore, the usage of cooperative communications significantly improve the performance of the considered system. We also pointed out that, by using a number of transmit antennas at the power beacon equal to the number of receive antennas at gateways, the best performance of the considered EH-LPWA system can be achieved.

ACKNOWLEDGMENT

This publication is the output of the ASEAN IVO (http://www.nict.go.jp/en/asean_ivo/index.html) project, "An energy efficient, self-sustainable, and long range IoT system for drought monitoring and early warning", and financially supported by NICT (http://www.nict.go.jp/en/index.html).

DATA AVAILABILITY

The data used to support the findings of this study are available from the corresponding author upon request.

CONFLICTS OF INTEREST

The authors declare that they have no conflicts of interest.

REFERENCES

[1] B. Clerckx, R. Zhang, R. Schober, D. W. K. Ng, D. I. Kim, and H. V. Poor, "Fundamentals of wireless information and power transfer: From RF energy harvester models to signal and system designs," *IEEE Journal on Selected Areas in Communications*, vol. 37, no. 1, pp. 4–33, 2018.

[2] Q.-V. Pham, F. Fang, V. N. Ha, M. J. Piran, M. Le, L. B. Le, W.-J. Hwang, and Z. Ding, "A survey of multi-access edge computing in 5G and beyond: Fundamentals, technology integration, and state-of-the-art," *IEEE Access*, vol. 8, pp. 116 974–117 017, 2020.

[3] X. Lu, P. Wang, D. Niyato, D. I. Kim, and Z. Han, "Wireless networks with RF energy harvesting: A contemporary survey," *IEEE Communications Surveys & Tutorials*, vol. 17, no. 2, pp. 757–789, 2014.

[4] V.-D. Nguyen, T. Q. Duong, H. D. Tuan, O.-S. Shin, and H. V. Poor, "Spectral and energy efficiencies in full-duplex wireless information and power transfer," *IEEE Transactions on Communications*, vol. 65, no. 5, pp. 2220–2233, 2017.

[5] Z. Ni and M. Motani, "Performance of energy harvesting receivers with power optimization," *IEEE Transactions on Communications*, vol. 66, no. 3, pp. 1309–1321, 2018.

[6] H. Ko and S. Pack, "A software-defined surveillance system with energy harvesting: Design and performance optimization," *IEEE Internet of Things Journal*, vol. 5, no. 3, pp. 1361–1369, 2018.

[7] B. C. Nguyen, X. N. Tran *et al.*, "On the performance of roadside unit-assisted energy harvesting full-duplex amplify-and-forward vehicle-to-vehicle relay systems," *AEU-International Journal of Electronics and Communications*, p. 153289, 2020.

[8] Y. Alsaba, C. Y. Leow, and S. K. A. Rahim, "Full-duplex cooperative non-orthogonal multiple access with beamforming and energy harvesting," *IEEE Access*, vol. 6, pp. 19 726–19 738, 2018.

[9] Y. Dong, M. J. Hossain, and J. Cheng, "Performance of wireless powered amplify and forward relaying over nakagami-m fading channels with nonlinear energy harvester," *IEEE Communications Letters*, vol. 20, no. 4, pp. 672–675, 2016.

[10] B. C. Nguyen, T. M. Hoang, P. T. Tran, and T. N. Nguyen, "Outage probability of NOMA system with wireless power transfer at source and full-duplex relay," *AEU - International Journal of Electronics and Communications*, vol. 116, p. 152957, 2020.

[11] M. Babaei, Ü. Aygölü, M. Başaran, and L. Durak-Ata, "BER performance of full-duplex cognitive radio network with nonlinear energy harvesting," *IEEE Transactions on Green Communications and Networking*, vol. 4, no. 2, pp. 448–460, 2020.

[12] A. Koc, I. Altunbas, and E. Basar, "Two-way full-duplex spatial modulation systems with wireless powered AF relaying," *IEEE Wireless Communications Letters*, vol. 7, no. 3, pp. 444–447, 2018.

[13] P. Deng, B. Wang, W. Wu, and T. Guo, "Transmitter design in MISO-NOMA system with wireless-power supply," *IEEE Communications Letters*, vol. 22, no. 4, pp. 844–847, 2018.

[14] M. A. Karami and D. J. Inman, "Linear and nonlinear energy harvesters for powering pacemakers from heart beat vibrations," in *Active and Passive Smart Structures and Integrated Systems 2011*, vol. 7977. International Society for Optics and Photonics, 2011, p. 797703.

[15] Z. Wei, S. Sun, X. Zhu, D. I. Kim, and D. W. K. Ng, "Resource allocation for wireless-powered full-duplex relaying systems with nonlinear energy harvesting efficiency," *IEEE Transactions on Vehicular Technology*, vol. 68, no. 12, pp. 12 079–12 093, 2019.

[16] F. Gu, J. Niu, L. Jiang, X. Liu, and M. Atiquzzaman, "Survey of the low power wide area network technologies," *Journal of Network and Computer Applications*, vol. 149, p. 102459, 2020.

[17] M. Bembe, A. Abu-Mahfouz, M. Masonta, and T. Ngqondi, "A survey on low-power wide area networks for iot applications," *Telecommunication Systems*, vol. 71, no. 2, pp. 249–274, 2019.

[18] O. Georgiou and U. Raza, "Low power wide area network analysis: Can lora scale?" *IEEE Wireless Communications Letters*, vol. 6, no. 2, pp. 162–165, 2017.

[19] M. Centenaro and L. Vangelista, "Time-power multiplexing for LoRa-based IoT networks: An effective way to boost LoRaWAN network capacity," *International Journal of Wireless Information Networks*, vol. 26, no. 4, pp. 308–318, 2019.

[20] U. Raza, P. Kulkarni, and M. Sooriyabandara, "Low power wide area networks: An overview," *IEEE Communications Surveys & Tutorials*, vol. 19, no. 2, pp. 855–873, 2017.

[21] L. Parri, S. Parrino, G. Peruzzi, and A. Pozzebon, "Low power wide area networks (lpwan) at sea: Performance analysis of offshore data transmission by means of lorawan connectivity for marine monitoring applications," *Sensors*, vol. 19, no. 14, p. 3239, 2019.

[22] C. S. You, J. S. Yeom, and B. C. Jung, "Performance analysis of cooperative low-power wide-area network for energy-efficient b5g systems," *Electronics*, vol. 9, no. 4, p. 680, 2020.

[23] T. Sanislav, G. D. Mois, S. Zeadally, and S. C. Folea, "Energy harvesting techniques for internet of things (iot)," *IEEE Access*, vol. 9, pp. 39 530–39 549, 2021.

[24] H. Elahi, K. Munir, M. Eugeni, S. Atek, and P. Gaudenzi, "Energy harvesting towards self-powered iot devices," *Energies*, vol. 13, no. 21, p. 5528, 2020.

[25] T. Sanislav, S. Zeadally, G. D. Mois, and S. C. Folea, "Wireless energy harvesting: Empirical results and practical considerations for internet of things," *Journal of Network and Computer Applications*, vol. 121, pp. 149–158, 2018.

[26] P. Kamalinejad, C. Mahapatra, Z. Sheng, S. Mirabbasi, V. C. Leung, and Y. L. Guan, "Wireless energy harvesting for the internet of things," *IEEE Communications Magazine*, vol. 53, no. 6, pp. 102–108, 2015.

[27] A. Jeffrey and D. Zwillinger, *Table of integrals, series, and products*. Academic Press, 2007.

[28] B. C. Nguyen, N. N. Thang, X. N. Tran *et al.*, "Impacts of imperfect channel state information, transceiver hardware, and self-interference cancellation on the performance of full-duplex MIMO relay system," *Sensors*, vol. 20, no. 6, p. 1671, 2020.

[29] A. Goldsmith, *Wireless communications*. Cambridge university press, 2005.

[30] X. Wang, "A study of harvested power and energy harvesting efficiency using frequency response analyses of power variables," *Mechanical Systems and Signal Processing*, vol. 133, p. 106277, 2019.

[31] N.-P. Nguyen, H. Q. Ngo, T. Q. Duong, H. D. Tuan, and D. B. da Costa, "Full-duplex cyber-weapon with massive arrays," *IEEE Transactions on Communications*, vol. 65, no. 12, pp. 5544–5558, 2017.

[32] A. A. Nasir, X. Zhou, S. Durrani, and R. A. Kennedy, "Relaying protocols for wireless energy harvesting and information processing," *IEEE Transactions on Wireless Communications*, vol. 12, no. 7, pp. 3622–3636, 2013.

[33] Z. Yan, S. Chen, X. Zhang, and H. L. Liu, "Outage performance analysis of wireless energy harvesting relay-assisted random underlay cognitive networks," *IEEE Internet of Things Journal*, vol. 5, no. 4, pp. 2691–2699, 2018.